Artificial Neural Network Control of a Nonminimum Phase, Single-Flexible-Link

A. Register

W. Book

C.O. Alford

Georgia Institute of Technology
GTRI
Atlanta, GA 30332

Georgia Institute of Technology
School of ME
Atlanta, GA 30332

Georgia Institute of Technology
School of EE
Atlanta, GA 30332

Abstract

A single-link flexible manipulator with a rotary actuator at one end and a mass at the other is modeled using the Lagrangian method coupled with an assumed modes vibration model. A SIMO state space model is developed by linearizing the equations of motion and simplified by neglecting natural damping. Laplace domain pole-zero plots between torque input and tip position show nonminimum phase behavior. Nonminimum phase behavior causes difficulty for both conventional and artificial neural network (ANN) inverse-model control. The most promising ANN method for the control of flexible manipulators does not appear to converge to a solution when the system is lightly damped. To overcome this limitation, a modified cost function is proposed. Simulations show that the ANN is able to converge to a solution even in the case of no damping. The modified approach fails, however, for beams exceeding some critical length measure. Identification of the critical length and proposals for extending the result are discussed.

1. INTRODUCTION

Although the first study of artificial neural network (ANN) learning by McCulloch and Pitts occurred over 50 years ago, the use of ANNs did not become popular until more recently. Researchers have applied a variety of ANN technology to the control of mechanical structures and survey papers specifically related to ANN control of rigid mechanical systems may be found in the literature (e.g., [1]). The use of ANN learning control for flexible manipulators has also been studied, although less extensively.

A three-layer perceptron has been used to control a four-bar mechanism through a flexible coupling[2]. Flexible joint manipulators, however, do not exhibit nonminimum phase behavior so the results for flexible joint manipulators are not directly applicable to flexible link manipulators. A recurrent, three-layer perceptron has been used to control a scale model of a space-based, flexible manipulator with both joint and link flexibility[3]. The investigation, however, used low-pass filters and small gain constants to prevent excitation of vibration modes. In addition, no strain or tip measurements were used as inputs to the ANN controller. Thus, the experiment was an extension of the rigid link case. A multi-layer perceptron has been used for payload identification and gain selection for the control of a single-link flexible manipulator[4]. The ANN is not used as a controller but rather as a pattern classifier. Once the payload is identified and a gain selected, the linear control law does not change until the payload changes. An array of four multi-layer perceptrons has been used to manipulate a simulated flexible plate[5]. The simulated plate included gravity effects, and beam shape information was provided to the ANN using a novel gripper design. A multi-layer perceptron has also been used to control the tip-position of a single-link flexible manipulator[6]. The proposed ANN controller is relatively unconventional with a strong reliance on an external teacher, an ANN structure of sparse interconnects, and a linear activation function. No strain or tip measurements are used by the ANN and the results include only limited simulations.

The most promising research for ANN based flexible manipulator control used a multi-layer perceptron to control the tip position of a single-link flexible manipulator[7]. The investigation used an ANN controller with access to both traditional state measurements and strain measurements. The network consisted of one hidden layer with a surprisingly small number of units. Comparison with a fixed-gain controller showed advantages for the multi-layer perceptron.

Here, the ANN method proposed in [7] is extended to a more general case of a single-link flexible manipulator with light damping. A dynamic model is developed and reduced to a simplified pole-zero plot in the Laplace domain. In order to control the simplified model, a modified cost function is proposed. The modified cost function adds an additional gain to provide closed-loop damping. The addition of a damping term should allow

the modified method to be applied to a wider range of mechanisms.

2. EQUATIONS OF MOTION

A problem that must be considered when replacing rigid links with flexible links is that of characterizing and modeling the significant vibration modes that exist in a flexible manipulator. Three methods have been used to characterize the vibration: lumped-parameter, assumed-modes and finite-element. Each method has advantages and limitations. Here, the assumed-modes method is considered. The assumed-modes method, coupled with a Lagrangian technique, yields a recursive, closed-form, dynamic solution suitable for control purposes[8].

2.1. Natural Frequencies

With the assumed-modes method, natural frequencies and the deformed shape can be determined by applying the appropriate boundary conditions[9]. Boundary conditions consisting of hub inertia and load mass are sufficiently complex to demonstrate nonminimum phase behavior. Using Bernoulli-Euler beam assumptions, the normalized natural frequencies of a flexible link with inertia-mass boundary conditions may be determined. The normalized mode frequency may be expressed in radians-per-second by proper application of the physical parameters. After solving for natural frequencies, admissible mode shapes may be determined. By combining the set of admissible mode shapes with a set of time-dependent generalized coordinates, the one dimension vibration equation is obtained. Vibration displacement, which depends on both the position along the beam and time, is given by,

$$z(\xi, t) = \sum_n \psi_n(\xi)\phi_n(t), \qquad (1)$$

where $z(\xi, t)$ is the displacement away from the undeformed shape, $\psi_n(\xi)$ is the mode shape for the nth mode and $\phi_n(t)$ is the generalized coordinate for the nth mode. The time dependent displacement in Eqn. 1 is used to develop the dynamic equations of motion.

2.2. Dynamic Equations

The inverse dynamic equations of a manipulator can be used to determine the torque required to cause the manipulator to follow a specific trajectory. Theoretically, if the desired trajectory were known, the inverse dynamic equations could be solved for torque in an open-loop manner. Unfortunately, the transformations between a desired tip trajectory and the required rigid body and

flexible mode trajectories are not easy to determine. Under certain assumptions, it is possible to rearrange the inverse dynamic equations so that the desired tip trajectory can be used to drive the system.

There are several methods which can be used to find the inverse dynamic equations. Here, the Lagrangian method is used since the method gives more insight into the sensitivity of the model to changes in parameter values. Details of the Lagrangian method may be found in introductory mechanics texts[10]. Additional details using homogenous transformation matrices in the framework of the Lagrangian method may be found in robotics texts[11]. Finally, application of the assumed-modes vibration description to the Lagrangian method can be found in the literature[8].

Systematic application of the Lagrangian and a two mode vibration assumption yield an inverse dynamic equation of the form,

$$\begin{bmatrix} \tilde{N}_0 & \tilde{A}_1 & \tilde{A}_2 \\ \tilde{A}_1 & \tilde{N}_1 & 0 \\ \tilde{A}_2 & 0 & \tilde{N}_2 \end{bmatrix} \begin{bmatrix} \ddot{\theta} \\ \ddot{\phi}_1 \\ \ddot{\phi}_2 \end{bmatrix} + \begin{bmatrix} 0 & 0 & 0 \\ 0 & K_1 & 0 \\ 0 & 0 & K_2 \end{bmatrix} \begin{bmatrix} \theta \\ \phi_1 \\ \phi_2 \end{bmatrix} = \begin{bmatrix} 1 \\ \tilde{\psi}'_1(0) \\ \tilde{\psi}'_2(0) \end{bmatrix} \tau , \quad (2)$$

where,

$$\tilde{N}_0 \approx J_0 + \tfrac{1}{3}\rho A L^3 + m_l L^2 ,$$

$$\tilde{N}_n = J_0 \psi'_n(0)^2 + \rho A L \int_0^1 (\psi_n(\xi))^2 d\xi ,$$

$$\tilde{A}_n = J_0 \psi'_n(0) + \rho A L^2 \int_0^1 \xi \psi_n(\xi) d\xi ,$$

$$K_n = \tfrac{EI}{L^3} \int_0^1 \psi''_n(\xi)^2 d\xi ,$$

θ is the rigid body angle (not necessarily the hub angle), τ is the actuator torque, and $\tilde{\psi}'_i(0) = \frac{\psi'_i(0)}{L}$. Simplifying assumptions, $\psi'_1(0)\psi'_2(0) \approx 0$, $\dot{\theta}^2 \approx 0$, $\dot{\phi}_i \dot{\phi}_j \approx 0$, $\dot{\theta}\dot{\phi}_n \approx 0$, have been included in Eqn. 2. In this particular case, neglecting the second order, nonlinear terms is acceptable since the primary interest is to extract the nonminimum phase behavior. Over dot and over double-dot represent the derivative with respect to time and the second derivative with respect to time, respectively. Prime and double-prime represent the derivative with respect to length along the beam and second derivative with respect to length along the beam, respectively. The resulting state-space model is given by Eqn. 3, where y_H is the hub position, y_T is the tip position, and $|M|$ is the determinant of the mass matrix from Eqn. 2. It is important to note that pole locations do not depend on the choice of output. Zero locations, however, depend on the choice of output, so that nonminimum phase behavior occurs only with the appropriate choice of output.

2.3. Generic Manipulator Parameters

Specific parameters are chosen to correspond to reasonable values for single link flexible manipulator discussions found in the literature. The parameters are not specific to any particular manipulator. The selected values are: $J_0 = 0.01 \text{ Nms}^2$, $\rho = 2700 \frac{\text{Kg}}{\text{m}^3}$, $w = 0.001 \text{ m}$, $h = 0.02 \text{ m}$, $m_l = 0.05 \text{ Kg}$, and $E = 71.0 \times 10^9 \text{ Pa}$. Applying beam parameters and finding the first four natural frequencies, results in the curves given in Figure 1. As the beam becomes longer, natural frequencies become smaller, allowing high order modes (e.g., 2nd, 3rd, etc.) to add important contributions to the vibration displacement. For long beams, it is probably not acceptable to follow the standard practice of considering only the first mode when designing a controller.

right-half plane poles is to allow non-causal solutions[12][13].

The number of zeros appearing in the RHP depends on the physical parameters of the beam. In this example, as the beam length increases, zeros move from the $j\omega$ axis to the real axis, compounding the problem of finding a suitable control model. For the generic manipulator, the point where the second pair of zeros moves to the real-axis occurs at a length of approximately 1.2 m. In previous artificial neural network methods, the nonminimum phase zero problem is not encountered due to either judicious or providential selection of the physical parameters[7]. A more general ANN controller, however, should be capable of controlling beams with an arbitrary distribution of system poles and zeros.

$$
\begin{bmatrix} \dot{\theta} \\ \dot{\phi}_1 \\ \dot{\phi}_2 \\ \ddot{\theta} \\ \ddot{\phi}_1 \\ \ddot{\phi}_2 \end{bmatrix} =
\begin{bmatrix}
0 & 0 & 0 & 1 & 0 & 0 \\
0 & 0 & 0 & 0 & 1 & 0 \\
0 & 0 & 0 & 0 & 0 & 1 \\
0 & \frac{\tilde{A}_1 \tilde{N}_2 K_1}{|M|} & \frac{\tilde{A}_2 \tilde{N}_1 K_2}{|M|} & 0 & 0 & 0 \\
0 & \frac{\tilde{A}_2^2 K_1 - \tilde{N}_0 \tilde{N}_2 K_1}{|M|} & -\frac{\tilde{A}_1 \tilde{A}_2 K_2}{|M|} & 0 & 0 & 0 \\
0 & -\frac{\tilde{A}_1 \tilde{A}_2 K_1}{|M|} & \frac{\tilde{A}_1^2 K_2 - \tilde{N}_0 \tilde{N}_1 K_2}{|M|} & 0 & 0 & 0
\end{bmatrix}
\begin{bmatrix} \theta \\ \phi_1 \\ \phi_2 \\ \dot{\theta} \\ \dot{\phi}_1 \\ \dot{\phi}_2 \end{bmatrix} +
\begin{bmatrix}
0 \\
0 \\
0 \\
\frac{\tilde{N}_1 \tilde{N}_2 - \tilde{A}_1 \tilde{N}_2 \tilde{\psi}_1'(0) - \tilde{A}_2 \tilde{N}_1 \tilde{\psi}_2'(0)}{|M|} \\
\frac{\tilde{N}_0 \tilde{N}_2 \tilde{\psi}_1'(0) + \tilde{A}_1 \tilde{A}_2 \tilde{\psi}_2'(0) - \tilde{A}_1 \tilde{N}_2 - \tilde{A}_2^2 \tilde{\psi}_1'(0)}{|M|} \\
\frac{\tilde{A}_1 \tilde{A}_2 \tilde{\psi}_1'(0) + \tilde{N}_0 \tilde{N}_1 \tilde{\psi}_2'(0) - \tilde{A}_2 \tilde{N}_1 - \tilde{A}_1^2 \tilde{\psi}_2'(0)}{|M|}
\end{bmatrix} \tau
$$

$$ \text{(3)} $$

$$
\begin{bmatrix} y_H \\ y_T \end{bmatrix} =
\begin{bmatrix}
1 & \psi_1'(0) & \psi_2'(0) & 0 & 0 & 0 \\
1 & \frac{\psi_1(1)}{L} & \frac{\psi_2(1)}{L} & 0 & 0 & 0
\end{bmatrix}
\begin{bmatrix} \theta \\ \phi_1 \\ \phi_2 \\ \dot{\theta} \\ \dot{\phi}_1 \\ \dot{\phi}_2 \end{bmatrix}
$$

Pole-zero plots of the transfer function between input torque and output tip position for two specific beam lengths are shown in Figure 2 and Figure 3. Poles lie on the $j\omega$ axis because damping has been neglected. The pair of poles at the origin are related to rigid-body motion and the remaining poles and zeros are related to vibration. Comparing pole locations, reiterates the inverse relationship between beam length and natural frequency.

While free vibration frequency is related to pole location, vibration phase is related to the zero location. Most importantly, right-half-plane (RHP) zeros occur in this model. The RHP zeros are responsible for the resulting nonminimum phase behavior. The RHP zeros are troublesome for certain types of inverse model control. An inverse may be found by replacing each system pole with a zero and each system zero with a pole, resulting in RHP poles and an unstable control model. One conventional method used to compensate for the resulting

3. MODIFIED ERROR FUNCTION

The ANN control method of [7] may be extended to lightly damped systems by adding a term related to the hub velocity to the cost function. The effect of the term is to increase the total system damping. The proposed cost function, minimized by ANN learning, is,

$$ J_{a,k} = \frac{1}{2} \left\{ Q e_{tip,k}^2 + R \tau_{k-1}^2 + S \hat{v}_{hub,k}^2 \right\}, \tag{4} $$

where, $e_{tip} = y_{desired} - y_{tip}$, and $\hat{v}_{hub}$ is an approximation of the hub velocity. The recurrence relationship for the approximation is,

$$ x_{0,k+1} = -x_{0,k} + \frac{2}{T} y_{hub,k} $$
$$ \hat{v}_{hub,k} = -2x_{0,k} + \frac{2}{T} y_{hub,k} \tag{5} $$

The relationships in Eqns. 4 and 5 may be used to find the total error. Individual error terms can be rewritten as,

$$e_{tip,k} = y_{desired,k} - C_2Ax_{k-1} - C_2B\tau_{k-1}, \quad (6)$$

$$\hat{v}_{hub,k} = -2\left(-x_{0,k-1} + \frac{2}{T}(C_1Ax_{k-2} + C_1B\tau_{k-2})\right) + \frac{2}{T}(C_1Ax_{k-1} + C_1B\tau_{k-1}) \quad (7)$$

where C_1 and C_2 are the first and second rows, respectively, of the output matrix in Eqn. 3.

In order to apply backpropagation, the weight change relationship in the output layer is the derivative chain given by,

$$\frac{\partial J_{a,k}}{\partial w_{oh,k-1}} = \frac{\partial J_{a,k}}{\partial \tau_{k-1}} \frac{\partial \tau_{k-1}}{\partial w_{oh,k-1}}. \quad (8)$$

The difference between the derivative chain in Eqn. 8 and standard backpropagation is that the derivative of the cost function is used instead of the normal backpropagation error term, $(o_d - o)$. Using Eqns. 6, and 7, the derivative of the cost function is,

$$\frac{\partial J_{a,k}}{\partial \tau_{k-1}} = -QC_2Be_{tip,k} + R\tau_{k-1} + \frac{2}{T}SC_1B\hat{v}_{hub,k}. \quad (9)$$

The value obtained by evaluating Eqn. 9 is used as the output layer's error. Similar to [7], in order for the control method to be effective, the ANN learning rate, and the error coefficients Q, R, and S must be carefully tuned.

To demonstrate the efficacy of the modified cost function, a 9-8-1 feedforward ANN is used. Units in both the hidden layer and the output layer use a hyperbolic tangent activation function. Learning is performed after every sample using the standard backpropagation-of-errors method (BackProp). An inertia term is not added to the BackProp algorithm. The structure of the ANN is consistent with [7] except for the use of sine and cosine on the angular input terms. A block diagram of the ANN controller and the simulation model is shown in Figure 4.

If damping is added to the model and the system is simulated, results similar to [7] are obtained. For comparison with [7], a plot of tip position versus time with gains $C_2B=1$, $Q=R=1$, and $S=0$ is shown in Figure 5. Note that by selecting $C_2B=1$, the characteristics of the plant in the cost function are assumed to be unknown. For the plot in Figure 5, the plant is simulated as a continuous model, using a 4th order Runge-Kutta integration method and a sub-step sample period of 0.25 ms. Consistent with [7], the ANN controller and the control torque are updated at a sample period of 8 ms.

If model damping terms are set to zero and S=0, a combination of values for Q, R, and the ANN learning parameter that allow the controller of [7] to converge could not be found. Additional simulations with relatively small damping terms were found to converge, however,

the resulting tip motion had large overshoot and prolonged oscillation. Adjusting parameters and allowing the ANN to learn over long periods of time did not appreciably reduce the overshoot and oscillations. The cost function from Eqn. 4, however, allows an ANN to control a plant with no damping. A plot of tip position versus time with gains $C_1B=C_2B=1$, Q=R=1, and S=0.2 is shown in Figure 6. The plant used to produce Figure 6 is identical to the plant used to produce Figure 5, except there is no damping in the plant model.

Since the pole-zero locations for any generic beam shorter than 1.2 m are similar to the 0.4 m case, it is expected that proper selection of gains and use of the modified cost function will provide good compensation. As expected, the modified cost function of Eqn. 4 works relatively well for generic beams up to approximately 1.2 m in length. Figure 7 and Figure 8 show the plots of tip position versus time for a 0.8 m generic beam and a 1.2 m generic beam, respectively. Beyond this length, ANN control fails due in part to a loss in the ability of a single strain gauge to accurately predict tip position. The loss in predictive ability can be seen in Figure 9. Whether the loss in predictive ability is caused by the changing zero distribution or due to a change in the second natural frequency is a topic for further investigation. The use of more than one strain gauge may allow an accurate tip estimate to be used in the cost function. This and other possible failure mechanisms for longer beams and the modified cost method are currently under investigation. Preliminary simulations using the exact, model generated tip position in the cost function have not been promising. It appears that the second nonminimum phase zero causes excessive error when the tip initially moves in the opposite direction.

4. CONCLUSION

A model for a single-link flexible manipulator has been presented and converted to a distribution of poles and zeros in the Laplace domain. It has also been shown that the distribution of zeros results in a nonminimum phase system and that the distribution of zeros changes radically with a relatively small change about some critical length.

It has been implied that previously proposed methods fail to converge in the lightly damped case. The implication cannot be proven because there is not yet a definitive method for the selection of system parameters. Cost function gains, ANN learning parameters, activation function(s), number of ANN layers and number of units in each layer must be selected in an ad-hoc way based on experience. A reasonable attempt was made to find suitable gains in the lightly damped case. An exhaustive

search, however, was not attempted. Even if the proper gains could be found, there are compelling reasons to use the new cost function.

A new cost function that includes a term related to the hub velocity has been proposed and shown to be effective in simulation. By penalizing the hub velocity, the new cost function allows the amount of closed-loop damping to be adjusted. By adjusting the amount of damping, overshoot can be traded with rise-time in a manner similar to the trade-off in a standard linear controller. Analytical expressions for tuning the gains are not yet available. Currently, gains must be selected by trial and error.

Finally, it has been shown that a single strain gauge looses the ability to accurately predict tip position beyond some critical length. The critical length is identified as the length when the second pair of zeros moves from the jω-axis to the σ-axis. It is not yet known whether the failure of the ANN method beyond the critical length is due to the loss of predictive ability or whether some fundamental problem exists. Simulations based on the actual tip position are far from complete, however, preliminary results have not been encouraging.

References

[1] Hunt, K., Sbarbaro, D., Zbikowski, R. and Gawthorp, P., "Neural Networks for Control Systems - A Survey," *Automatica* 28(6), 1992, pp.1083-1112.

[2] Chang, S., Nair, S., "A New Neural Network Control Architecture for a Class of Nonlinear Dynamic Systems," *Proc. ACC*, 1993, pp.79-83.

[3] Newton, R, Xu, Y., "Neural Network Control of a Space Manipulator," *IEEE Control System Mag.*, 13(5), Dec. 1993, pp.14-22.

[4] Askew, C., Sundareslian, M. and Wang, F., "A Neural Network Pattern Classification Approach for Payload Adaptive Regulation of Flexible Manipulators," *Proc. ACC*, 1993, pp.2518-2519.

[5] Arai, F., Rong, L., and Fukuda, T., "Trajectory Control of Flexible Plate Using Neural Network," *IEEE Intl. Rob. and Auto. Conf.*, 1993, pp.155-160.

[6] Cetinkunt, S., Chiu, H., "A Study of Learning Controllers for Tip Position Control of a Flexible Arm Using Artificial Neural Networks," *ASME Modeling and Control of Compliant and Rigid Motion Systems*, DSC-31, 1991, pp.15-19.

[7] Takahashi, K. and Yamada, I., "Neural-Network-Based Learning Control of Flexible Mechanism with Application to a Single-Link Flexible Arm," *Proc. 1993 ASME WAM, Intelligent Cont. Sys.*, DSC-Vol. 48, 1993, pp. 95-104.

[8] Book, W.J., "Recursive Lagrangian Dynamics of Flexible Manipulator Arms," *Intl. J. of Robotics Research* 3(3), 1984, pp. 87-101.

[9] Register, A., "A Note on the Vibration of Generally Restrained, End-Loaded Beams," *J. of Sound and Vib.*, Vol. 72, No. 4, 1994, pp. 561-571.

[10] Paz, M., *Structural Dynamics*, Van Nostrand Reinhold Company Inc. 1985.

[11] Paul, R.P., *Robot Manipulators Mathematics, Programming and Control*, MIT Press, Cambridge, MA 1981.

[12] Kwon, D.-S. and Book, W.J., "Tracking control of a nonminimum-phase flexible manipulator," *Proc. ASME WAM, Modeling and Control of Compliant and Rigid Motion Systems*, DSC-Vol. 31, Dec. 1991, pp. 27-37.

[13] Bayo, E., and Moulin, H., "An Efficient Computation of the Inverse Dynamics of Flexible Manipulators in the Time Domain," *IEEE Intl. Rob and Auto. Conf.*, 1989, pp. 710-715.
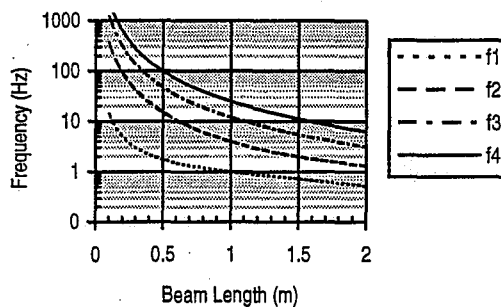
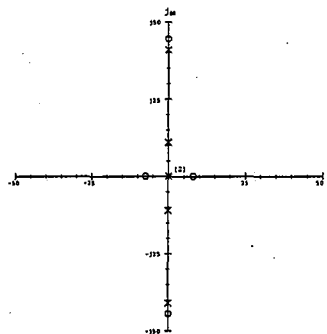Figure 1, natural frequency versus beam length.

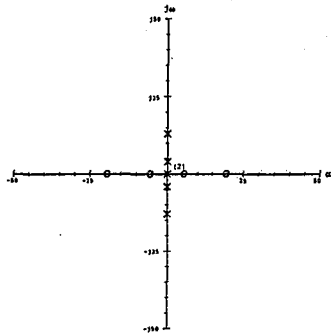Figure 2, tip pole-zero plot, length=0.8 m.
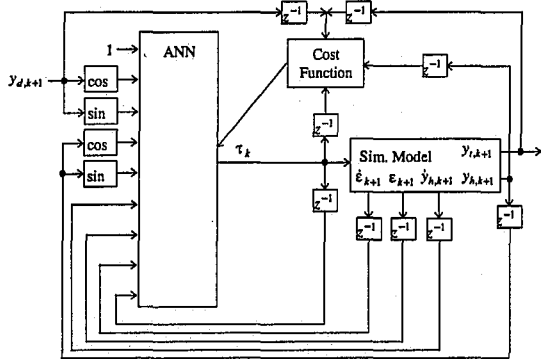
Figure 3, tip pole-zero plot, length=1.4 m.

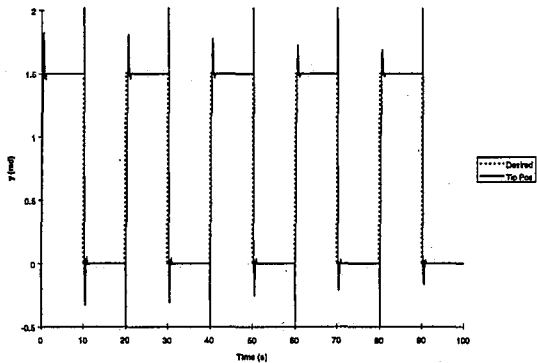Figure 4, block diagram of the system simulation with ANN controller.

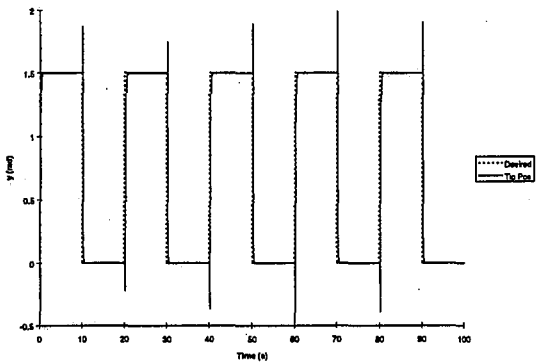Figure 5, plot of tip position versus time for 0.4 m beam, Q=R=1, S=0 and damping.

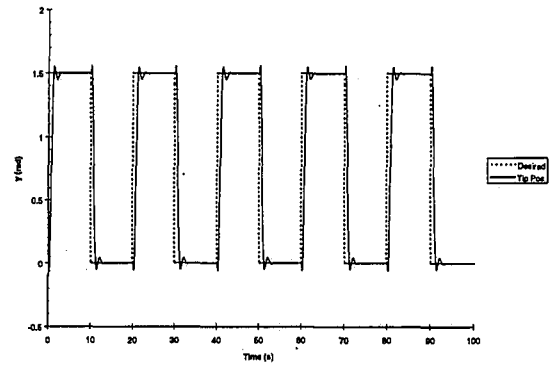Figure 6, plot of tip position versus time for 0.4 m beam, Q=R=1, S=0.2 and no damping

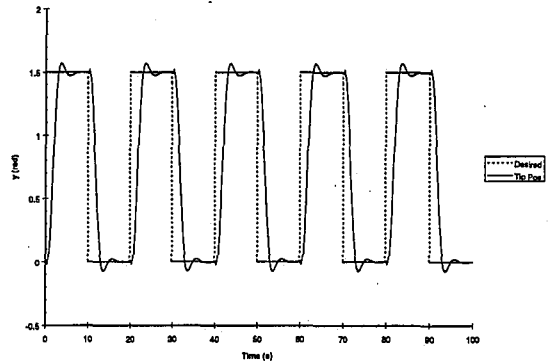Figure 7, plot of tip position versus time for 0.8 m beam, Q=0.25, R=1.0, V=0.175, no damping.

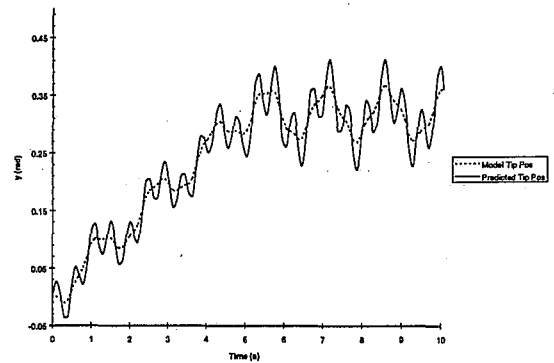Figure 8, plot of tip position versus time for 1.2 m beam, Q=0.15, R=1.6, V=0.25, no damping.

Figure 9, plots of model tip position and predicted tip position versus time for 1.4 m beam with a positive pulse input at t=0 s and negative pulse input at t=5 s.